AD-A053 232 LOWELL UNIV RESEARCH FOUNDATION MASS F/G 4/1
EFFECTS OF NON-THERMAL ELECTRONS ON THE MORPHOLOGY OF THE TOP-S--ETC(U)
NOV 77 M KANAL F19628-77-C-0065
UNCLASSIFIED ULRF-385/CAR AFGL-TR-77-0253 NL

| OF |
AD
A053232

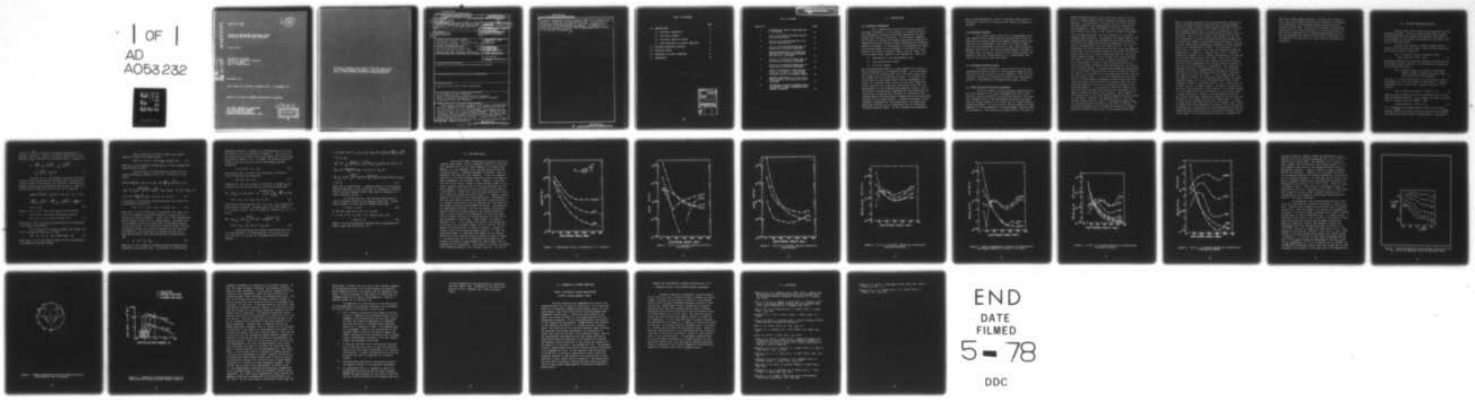

END
DATE
FILMED
5-78
DDC

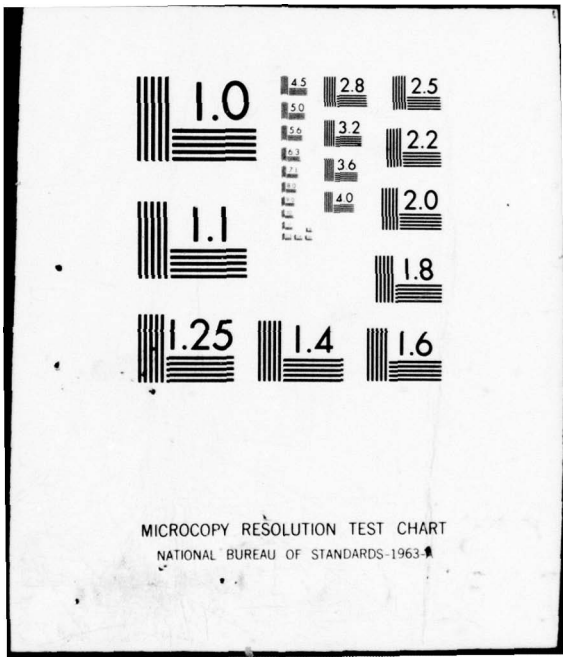
1.0
1.1
1.25
1.4
1.6
1.8
2.0
2.2
2.5
2.8
3.2
3.6
4.0
4.5
5.0
5.6
6.3
MICROCOPY RESOLUTION TEST CHART
NATIONAL BUREAU OF STANDARDS-1963-A

AFGL-TR-77-0253

EFFECTS OF NON-THERMAL ELECTRONS ON THE MORPHOLOGY OF THE TOP-SIDE IONOSPHERE

Madhoo Kanal

University of Lowell
Center for Atmospheric Research
450 Aiken Street
Lowell, Massachusetts

November 1977

Final Report for Period 1 December 1976 - 30 November 1977

AIR FORCE GEOPHYSICS LABORATORY
AIR FORCE SYSTEMS COMMAND
UNITED STATES AIR FORCE
HANSCOM AFB, MASSACHUSETTS 01731

UNCLASSIFIED

SECURITY CLASSIFICATION OF THIS PAGE (When Data Entered)

REPORT DOCUMENTATION PAGE	READ INSTRUCTIONS BEFORE COMPLETING FORM
1. REPORT NUMBER: AFGL-TR-77-0253	2. GOVT ACCESSION NO.
3. RECIPIENT'S CATALOG NUMBER	
4. TITLE (and Subtitle): EFFECTS OF NON-THERMAL ELECTRONS ON THE MORPHOLOGY OF THE TOP-SIDE IONOSPHERE.	5. TYPE OF REPORT & PERIOD COVERED: Scientific - Final rept. 1 Dec 76 - 30 Nov 77
	6. PERFORMING ORG. REPORT NUMBER: ULRF-385/CAR
7. AUTHOR(s): Madhoo Kanal	8. CONTRACT OR GRANT NUMBER(s): F19628-77-C-0065
9. PERFORMING ORGANIZATION NAME AND ADDRESS: University of Lowell, Center for Atmospheric Research, 450 Aiken Street, Lowell, Massachusetts 01854	10. PROGRAM ELEMENT, PROJECT, TASK AREA & WORK UNIT NUMBERS: 35160F 2311-G2-05
11. CONTROLLING OFFICE NAME AND ADDRESS: Air Force Geophysics Laboratory, Hanscom AFB, Massachusetts 01731, Contract Monitor: Michael Smiddy/PHR	12. REPORT DATE: November 1977
	13. NUMBER OF PAGES: 36 (12 35 pl.)
14. MONITORING AGENCY NAME & ADDRESS (if different from Controlling Office)	15. SECURITY CLASS. (of this report): Unclassified
	15a. DECLASSIFICATION/DOWNGRADING SCHEDULE

16. DISTRIBUTION STATEMENT (of this Report)

Approved for public release; distribution unlimited.

17. DISTRIBUTION STATEMENT (of the abstract entered in Block 20, if different from Report)

18. SUPPLEMENTARY NOTES

Papers on this subject under preparation.

19. KEY WORDS (Continue on reverse side if necessary and identify by block number)

Hyperthermal Electron Transport
Electron Distribution in the Top-Side Ionosphere
Electron Transport Phenomenon in the Top-Side Ionosphere
Morphology of Electron Transport

20. ABSTRACT (Continue on reverse side if necessary and identify by block number)

This report contains a summary of the study of hyperthermal electron transport in the temperate, the precipitation and the polar regions of the top-side ionosphere. It accounts for the electron energy loss to the neutral atmospheric species and the continuous loss to the ambient thermal plasma. The pitch angle scattering of hyperthermal electrons by the neutral species and ambient plasma is taken into account. A basic equation of

DD FORM 1 JAN 73 1473 EDITION OF 1 NOV 65 IS OBSOLETE

UNCLASSIFIED

SECURITY CLASSIFICATION OF THIS PAGE (When Data Entered)

409 596

transport, analogous to the Boltzmann's type of an equation, was derived to obtain the distribution function. A discovery of a variational principle was made to deal with the empirically fitted data of the scattering experiments. A complete set of models was arrived at to treat the aforementioned three regions of the top-side ionosphere.

TABLE OF CONTENTS

LIST OF FIGURES

1.0 INTRODUCTION

1.1 Technical Background

For a comprehensive study of the ionized state of the upper atmosphere, it is necessary to consider all relevant fundamental processes which are responsible for maintaining that state of ionization. As the earth's magnetic field serves to confine the plasma, the electron density and temperature profiles exhibit marked differences for different magnetic latitudes. In consequence, to understand the dynamic processes which involve transport of electrons from one region of the earth to another region, one must make a distinction among three regions of the atmosphere. These are:

a) Equatorward of the precipitation zone.

b) The precipitation region.

c) The polar region.

The distinguishing features of these regions are related to the configurations of the magnetic fields. For the equatorward side of the precipitation zone, the field lines below the plasma pause are essentially closed. In contrast, the field lines in the precipitation zone are presumably connected to the plasma sheet, while, in the polar region the field lines may find a possible connection either with the magnetosphere or the interplanetary magnetic fields. One of the careful considerations engendered by these differing configurations in dealing with transport of electrons is the corresponding differing boundary conditions and the associated problems of the energy balance. A study and analysis of the transport phenomenon and the morphology of the upper atmosphere was carried out in cooperation with the Electrical Processes Branch of AFGL. In the following few sections we

give a brief exposition of some of the basic ideas that are involved in this kind of study and also sketch our method of approach.

1.2 The Basic Problem

For a given steady state flux of hyperthermal electrons whose initial energy spectrum is prescribed, if we assume that the neutral species and ambient plasma profiles are also given (or prescribed), then what is the final steady state of the hyperthermal electrons as they travel along the magnetic field lines? We allow the hyperthermal electrons to interact with the neutral species and the ambient plasma, but otherwise they are correlationless, i.e. hyperthermal electrons do not interact with each other.

1.3 The Basic Quantity Sought

The basic quantity we wish to find is the electron distribution function, which is, the expected number of electrons per cm^3 per electron volt per steradian. Once the distribution function is determined, then any other macroscopic quantity is determined by averaging with respect to that.

1.4 Some Problems of Interest Addressed

There are several relevant problems associated with the three regions of the upper atmosphere mentioned before. The basic question pertains to the energy balance of the spectral (energy) flux of the hyperthermal electrons associated with the energy budget of the neutral and the thermal ambient plasma environment. By that we mean that any amount of energy imparted to the environment by the hyperthermal electrons must be accountable. This energy may appear either in the form of

ambient plasma heating or excitation (also possible ionization) of neutral species with a possible subsequent optical emission. To elaborate on this point let us first consider the role played by the hyperthermal electrons produced by photoionization. About one-third of the solar energy spectrum between soft x-rays (~14Å) and EUV (~1100Å) is expended into the photoionization and (or) excitation of the atmospheric neutral species. In general, the energy range of the photoelectron fluxes lies between zero and 200 eV (electron volts) and the significant altitude range where they are produced is between about 120 km to about 400 km. In a real atmosphere, as these photoelectrons travel along the magnetic field lines, they lose their energy by collisions with neutral species and also by Coulomb interaction with the relatively cooler ambient plasma. The collisions with neutral species may result in excitation (and) or further ionization. If it is an excitational collision then the photoelectrons will lose their energy in discrete jumps determined by the excitation threshold energy. The excitation-energy may subsequently be lost by either optical emission (such as 6300Å red line of ^1O_D state) or be quenched by collisional deexcitation (such as N_2 vibrational states). If it is an ionizational collision then, the total energy of emerging electrons (which may have continuous energy distribution) plus whatever goes into excitation-energy of the ion, must balance the energy of the impacting electron. In consequence, there are several channels into which an impacting electron can distribute its energy in interaction with neutral species. With respect to the energy loss to the cooler ambient plasma, the loss process is continuous. However, the important point is that the Coulomb interaction will result in raising the ambient electron temperature more efficiently than that of the ions. As an specific example let us consider the transport of photoelectrons from the sunlit side to the conjugate dark side.

Some of the data analyzed from the electrostatic analyzer onboard the INJUN5 satellite exhibited that the hyperthermal electron fluxes, in the altitude range of 1000 km to 2500 km, with energies greater than 2 eV were a consequence of the photoelectrons which were transported from the sunlit side of the earth. Thus, in the accessed, dark-regions of the topside ionosphere, the observed temperatures were between 3000 to 4000°K with highest temperatures near the trough. The unaccessed regions were essentially isothermal with the temperature in the neighborhood of 2000°K. As a coauthor to W. J. Burke and R. C. Sagalyn, this study of observations has been submitted as a paper to J. Geophys. Res. (1977). Another interesting example of the transport phenomenon is the excitation of the stable auroral arcs (SAR). As is well known, during high K_p-indices the ring current protons move inward into the cool plasmasphere and the ring current is eroded by the cyclotron wave turbulence instability. The resulting transfer of energy to plasmaspheric electrons is conducted down into the lower ionosphere where the ambient electrons are heated to as much as 5000°K. If the energy density of the ambient electrons is sufficiently high (about 0.02 ergs) the high energy tail of the distribution will then contain sufficient number of electrons (about 2 eV) to excite the ^1O_D (6300Å) line of the atomic oxygen. Of course, the reaction rate will directly depend on the density of the atomic oxygen. For that reason SAR arcs are observed in the altitude range of about 250-600 km. However, the more important point is that here the transport phenomenon combines with the heat conduction and the energy source is the ring current. A paper on this subject has been submitted to J. Geophys. Res. (1977). To mention two other examples of interest, one is the secondary production of electrons and their distribution in the precipitation zone and the other is the escape of plasma in the polar region. In the precipitation zone, if we assume that

the flux of high energy electrons (1-50 keV) is of known nature, then this boundary condition is sufficient to determine the distribution (and secondary electron production rate) along the entire path. Here one can envisage an interesting possibility of an inverse problem, i.e. given the results of some rocket experiment in the auroral (precipitation) zone, can one determine the nature of the source of electrons? We investigated the possibility of such a type of data profile inversion.

2.0 ELECTRON TRANSPORT EQUATION

We now give a brief sketch of the derivation of the transport equation. From any closed volume fixed in space the electrons flow out, whereby the advective term equal to the divergence of the current contributes to the loss of electrons in the phase space.

The electron transport equation emerges when we balance the source and sink terms. Thus, we have the continuity equation which is given by

$$\text{Div. of Electron Current} + \text{Electron Sinks} = \text{Source Function} + \text{SES} + \text{PES} \tag{1}$$

where SES represents the secondary electron spectrum and PES the primary electron spectrum. We now define the photoelectron distribution (PED) as

$$\text{PED} = \text{expected number of electrons (excluding ambient plasma electrons) per unit volume per electron volt per steradian.} \tag{2}$$

Let $f(\underline{r}, E, \mu)$ denote PED, where $\underline{r}$ is the position vector, E the energy and μ the pitch angle of the electron. Various components of Eq. (1) are then, related to $f(\underline{r}, E, \mu)$ as follows:

$$\text{Div. of Electron Current} = \nabla \cdot \underline{u} f(\underline{r}, E, \mu) \tag{3}$$

where $\underline{u}$ is the velocity vector of the electron and ∇ is the spatial gradient operator. Let ν_t denote the total collision rate of electrons with the medium. Then

$$\text{Electron Sinks} = \nu_t f(r, E, \mu) \tag{4}$$

If n_I represents the number density (no/cm^3) of neutral species, $Q_{IJ}^{(ex)}(E)$ the cross-section for excitation and $Q_{IJ}^{(ion)}(E)$ the ionization cross-section corresponding to J-th state of

species I, $Q_I^{(e)}(E)$ the elastic scattering cross-section of species I and r(E) (= $\Delta E/\Delta t$) the rate of energy loss to the ambient plasma, then the total collision rate ν_t is given by

$$\nu_t = \sqrt{\frac{2E}{m}} \left[\sum_{I,J} n_I Q_{IJ}^{(ex)}(E) + \sum_{I,J} n_I Q_{IJ}^{(ion)}(E) + \sum_I n_I Q_I^{(e)}(E) \right] + \frac{1}{\Delta E} r(E) \quad (5)$$

Let $R(E', \underline{\Omega}' \rightarrow E, \underline{\Omega})$ generally represent the probability (or the redistribution function) that an electron of initial energy E' and momentum unit vector Ω' upon collision emerges with energy E and momentum unit vector Ω. Then the source function (emission term) in Eq. (1) is given by

$$\text{SOURCE FUNCTION} = \frac{1}{4\pi} \int_0^\infty dE' \int d\Omega' \, R(E', \underline{\Omega}' \rightarrow E, \underline{\Omega}) \left[\sqrt{\frac{2E'}{m}} \sum_I n_I Q_I^{(e)}(E') + \sqrt{\frac{2E'}{m}} \sum_{I,J} n_I Q_{IJ}^{(ex)}(E') + \frac{r(E')}{\Delta E'} \right] f(\underline{r}, E', \underline{\Omega}) \quad (6)$$

where m (= 9.1×10^{-28} gm) is the mass of the electron.

For elastic scattering from neutral species

$$R(E', \underline{\Omega}' \rightarrow E, \underline{\Omega}) = \delta(E'-E) \, R_e(\underline{\Omega}' \rightarrow \underline{\Omega}) \quad (7)$$

where $R_e(\underline{\Omega}' \rightarrow \underline{\Omega})$ is the angular phase function corresponding to the elastic scattering.

For scattering by plasma we assume that energy lost by the incident electron is ΔE. Then

$$R(E', \underline{\Omega}' \rightarrow E, \underline{\Omega}) = \delta(E'-E-\Delta E) \, R_p(\underline{\Omega}' \rightarrow \underline{\Omega}) \quad (8)$$

where $R_p(\underline{\Omega}' \rightarrow \underline{\Omega})$ is the angular phase function corresponding to scattering by ambient plasma.

For an inelastic collision in which the neutral species is left in an excited state,

$$R(E', \underline{\Omega}' \rightarrow E, \Omega) = \delta(E'-E-W_{IJ})\, R_{IJ}(\underline{\Omega}' \rightarrow \underline{\Omega}) \qquad (9)$$

where W_{IJ} is the threshold energy and R_{IJ} is the corresponding angular phase function.

Substituting the redistribution functions for the various processes as given by Eqs. (7) - (9) into Eq. (6) we obtain

$$\text{SOURCE FUNCTION} = \frac{1}{4\pi} \int d\Omega'\, R_e(\underline{\Omega}' \rightarrow \underline{\Omega}) \sqrt{\frac{2E}{m}} \sum_I n_I Q_I^{(e)} f(\underline{r}, E, \underline{\Omega}')$$

$$+ \frac{1}{4\pi} \int d\Omega' \sum_{IJ} \sqrt{\frac{2(E + W_{IJ})}{m}}\, n_I Q_{IJ}^{(ex)}(E + W_{IJ})\, R_{IJ}(\underline{\Omega}' \rightarrow \underline{\Omega})\, f(\underline{r}, E+W_{IJ}, \underline{\Omega}')$$

$$+ \frac{1}{4\pi} \int d\Omega' \frac{r(E + \Delta E)}{\Delta E} R_p(\underline{\Omega}' \rightarrow \underline{\Omega})\, f(\underline{r}, E + \Delta E, \underline{\Omega}') \,. \qquad (10)$$

To calculate the secondary electron spectrum let us write the redistribution function as

$$R(E', \underline{\Omega}' \rightarrow E, \underline{\Omega}) = \sigma(E' \rightarrow E)\, R_s(\underline{\Omega}' \rightarrow \underline{\Omega}) \qquad (11)$$

where $\sigma(E' \rightarrow E)$ is differential cross-section (cf. Opal et al, 1971) for producing a secondary electron of energy E by an electron of initial energy E'. $R_s(\underline{\Omega}' \rightarrow \underline{\Omega})$ is the corresponding angular phase function for the given process. We assume that in the primary electron spectrum (PES) the maximum energy of an electron is E_M. If an electron of initial energy E' has an ionizing collision with a neutral species with two electrons of energies E_p and E_S exiting, and ionized species left in some excited state, then the conservation of energy states that

$$E' = E_p + E_S + W_{IJ} \qquad (12)$$

where W_{IJ} is the ionization threshold plus the energy corresponding to the excited state. We now wish to know how many

secondary electrons of energy E_P are produced per cm^3 per sec per electron volt by electrons of energy E'. The value of E' may range from E_M to some lowest value permitted by the energy conservation equation (12). Evidently the second electron of energy E_S may end up in any part of the energy spectrum bounded by

$$0 \leq E_S \leq E_M - E_P - W_{IJ} \ . \tag{13}$$

This implies that in order for an ionization collision to occur E' must obey the inequality

$$E_P + W_{IJ} \leq E' \leq E_M \ . \tag{14}$$

Consequently, the total number of electrons of energy E_P produced per cm^3 per sec per electron volt per steradian are

$$SES = \frac{1}{4\pi} \sum_{IJ} n_I \int d\Omega' \, R_S(\underline{\Omega}' \to \underline{\Omega}) \int_0^{E_M - E_P - W_{IJ}} dE_S \int_{E_P + W_{IJ}}^{E_M} dE' \, \sqrt{\frac{2E'}{m}} \, \sigma(E' \to E_P)$$

$$\cdot \, \delta(E' - E_P - E_S - W_{IJ}) \, f(r, E', \Omega') \tag{15}$$

where Dirac's delta function $\delta(E' - E_P - E_S - W_{IJ})$ ensures the conservation of energy. Integration in (15) with respect to E' is rather trivial. With the change of variable $E_P + E_S = E''$, we get

$$SES = \frac{1}{4\pi} \sum_{I,J} n_I \int d\Omega' \int_{E_P}^{E_M - W_{IJ}} dE'' \, R_S(\underline{\Omega}' \to \underline{\Omega}) \sqrt{\frac{2}{m}} \, (E'' + W_{IJ})$$

$$\cdot \, \sigma(E'' + W_{IJ} \to E_P) \, f(\underline{r}, E'' + W_{IJ}, \underline{\Omega}') \ . \tag{16}$$

Now substituting the explicit expressions for various constituents of the continuity Eq. (1) as given by (3), (4), (10) and (16) we get the following electron transport equation

$$\nabla \cdot \underline{u}\, f(\underline{r}, E, \underline{\Omega}) + \nu_t\, f(\underline{r}, E, \underline{\Omega}) = \frac{1}{4\pi} \int d\Omega'\, R_e(\underline{\Omega}' \to \underline{\Omega}) \sqrt{\frac{2E}{m}} \sum_I n_I Q_I^{(e)}(E)$$

$$\cdot f(\underline{r}, E, \underline{\Omega}')$$

$$+ \frac{1}{4\pi} \int d\Omega' \sum_{I,J} \sqrt{\frac{2}{m}(E+W_{IJ})}\, n_I Q_{IJ}^{(ex)}(E+W_{IJ})\, R_{IJ}(\underline{\Omega}' \to \underline{\Omega})\, f(\underline{r}, E+W_{IJ}, \underline{\Omega}')$$

$$+ \frac{1}{4\pi} \int d\Omega' \frac{r(E+\Delta E)}{\Delta E} R_P(\underline{\Omega}' \to \underline{\Omega})\, f(\underline{r}, E+\Delta E, \underline{\Omega}')$$

$$+ \frac{1}{4\pi} \sum_{I,J} n_I \int d\Omega' \int_E^{E_M - W_{IJ}} dE'\, R_S(\underline{\Omega}' \to \underline{\Omega}) \sqrt{\frac{2}{m}(E'+W_{IJ})}\, \sigma(E'+W_{IJ} \to E) f(\underline{r}, E'+W_{IJ}, \underline{\Omega}')$$

$$+ P(E, \underline{r}) \qquad (17)$$

where $P(E, \underline{r})$ denotes PES. A simpler version of this equation has been discussed in the literature (cf. McCormick and Kuscer (1965), Case and Zweifel (1967), Mika (1961), Zelazny et al (1961) and Kanal (1970)).

In writing down Eq. (17), we have neglected the roles of electric field ($\underset{\sim}{\varepsilon}$) and magnetic field ($\underset{\sim}{B}$). In generals, however, one must add the Lorentz force term

$$\underset{\sim}{F} = q(\underset{\sim}{\varepsilon} + \underset{\sim}{u} \times \underset{\sim}{B}) \qquad (18)$$

to the left hand side of Eq. (17) so that

$$\nabla \cdot \underset{\sim}{u}\, f(\underset{\sim}{r}, E, \underset{\sim}{\Omega}) + \nu_t\, f(\underset{\sim}{r}, E, \underset{\sim}{\Omega}) + \frac{1}{m} \underset{\sim}{F} \cdot \nabla_u f(\underset{\sim}{r}, E, \underset{\sim}{\Omega})$$

$$= R_c(\underset{\sim}{r}, E, \underset{\sim}{\Omega}) \qquad (19)$$

where ∇_u is velocity gradient operator and R_c represents the entire right hand side of Eq. (17).

3.0 COMPLETED TASKS

For a pitch angle scattering of electrons, which is linearly anisotropic, we have complete solutions of the transport equation (17) for all three regions of the upper atmosphere, i.e. the temperate zone, the precipitation zone and the polar region. A computer program is available, which is adapted to the AFGL CDC 6600 computer. It was our original intention to run this program completely without any bugs and make a permanent file for AFGL's use. However, it was felt that for a four month's effort it would be more useful to construct complete theories first for the precipitation and the polar regions. This decision was dictated by the existence of the wealth of INJUN5 data and the anticipated data on electric fields and plasma bulk motion from R. C. Sagalyn's experiments on S3-2 and S3-3 Air Force Satellites. Furthermore, it was also felt that our model of pitch angle scattering which is, linearly anisotropic, was not adequate for the entire useful energy spectrum of hyperthermal electrons. For instance, for high energy electrons (>50 eV) the angular differential cross-sections are highly peaked in the forward direction. This is clearly seen in the experiments of Crooks and Rudd (1972) in which electrons of energy between 50 eV and 800 eV were bombarded on helium gas. Their results are shown in Figures 1 to 7. If we consider the elastic scattering first, we see that for all energy ranges (50 eV to 200 eV) the differential cross-sections, as shown in Figure 1, assume the largest values for scattering angles close to 0°. Here the scattering angle θ is measured with respect to the initial direction of the electron velocity vectors as shown in Figure 1. In particular, for 50 eV electrons the probability for forward scattering is approximately 20 times larger than the probability for backscatter. This factor, of course, increases with increasing energy of the incident electron. For an ex-

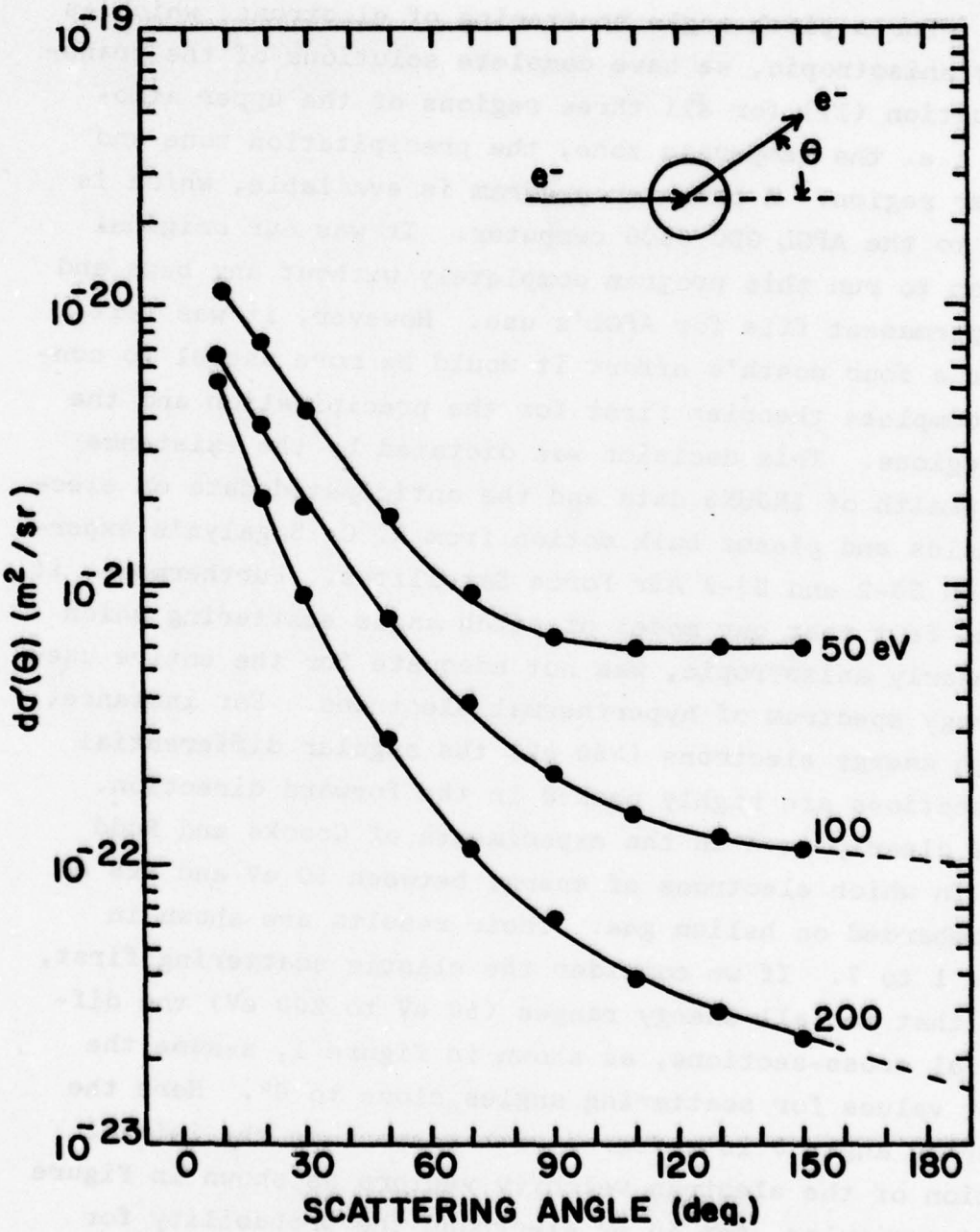

Figure 1. Differential Elastic Cross-Section, e^- on Helium

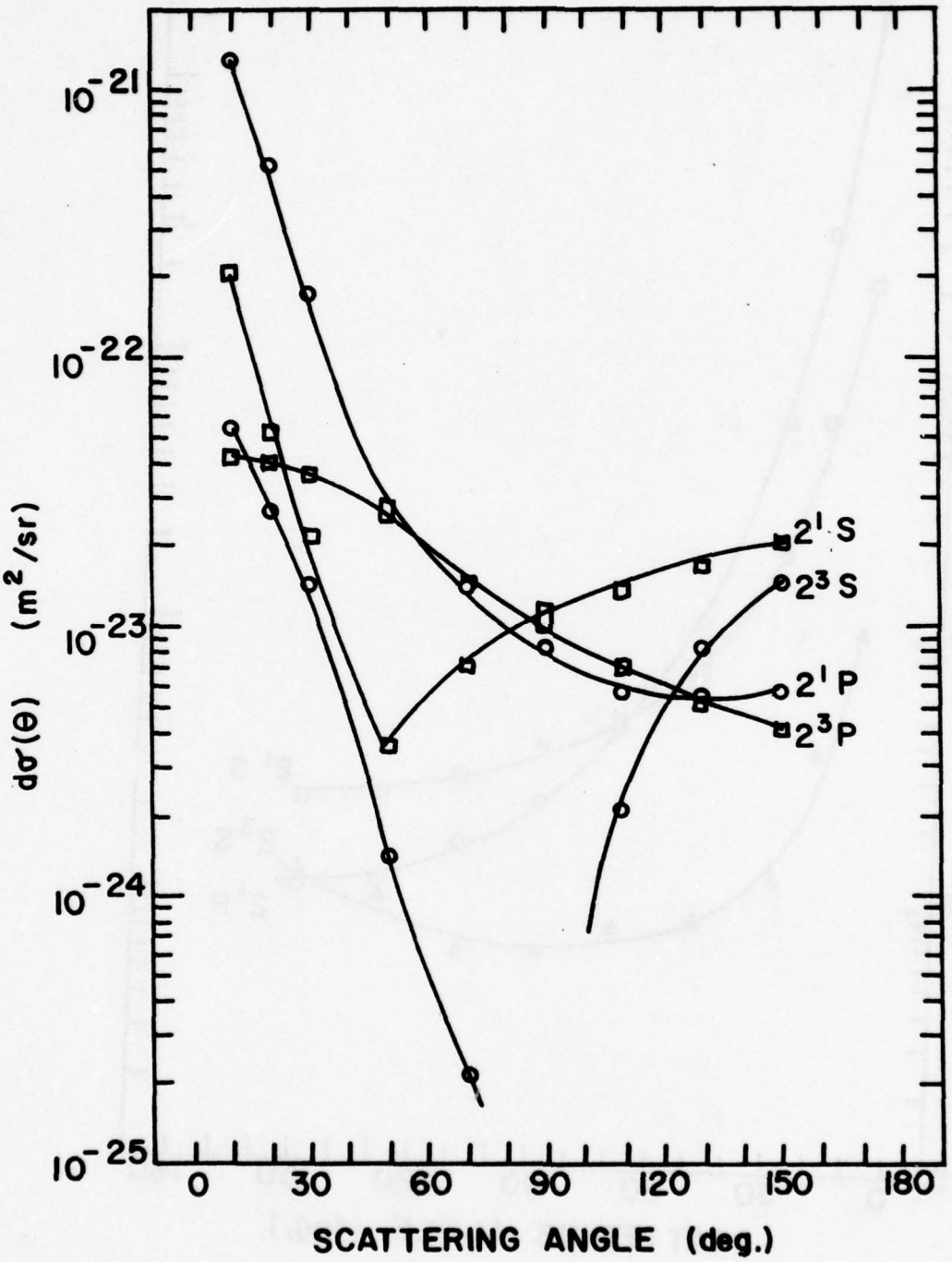

Figure 2. 50 eV e^- on Helium, Absolute Excitation Cross-Section.

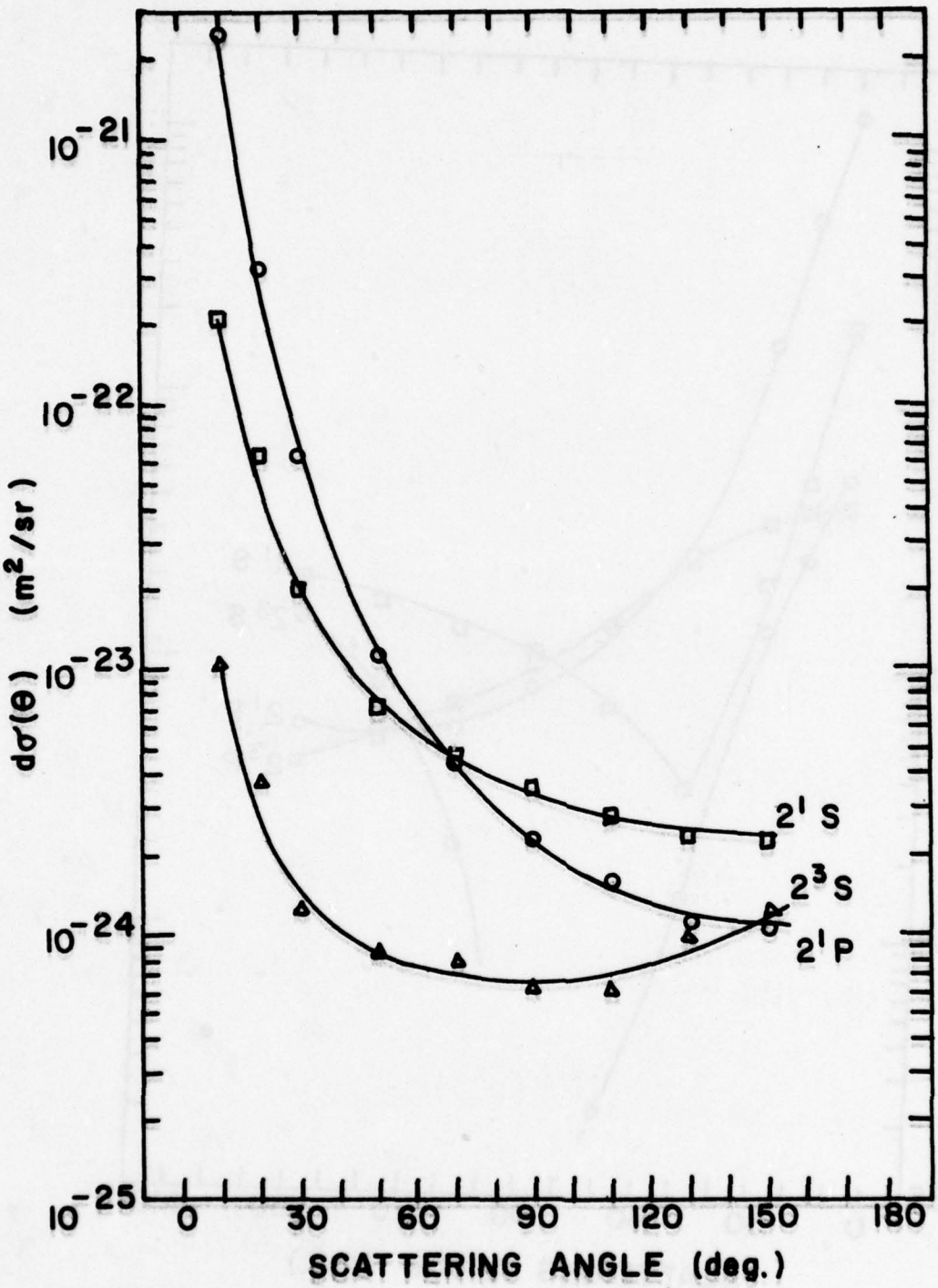

Figure 3. 100 eV e^- on Helium, Absolute Excitation Cross-Section.

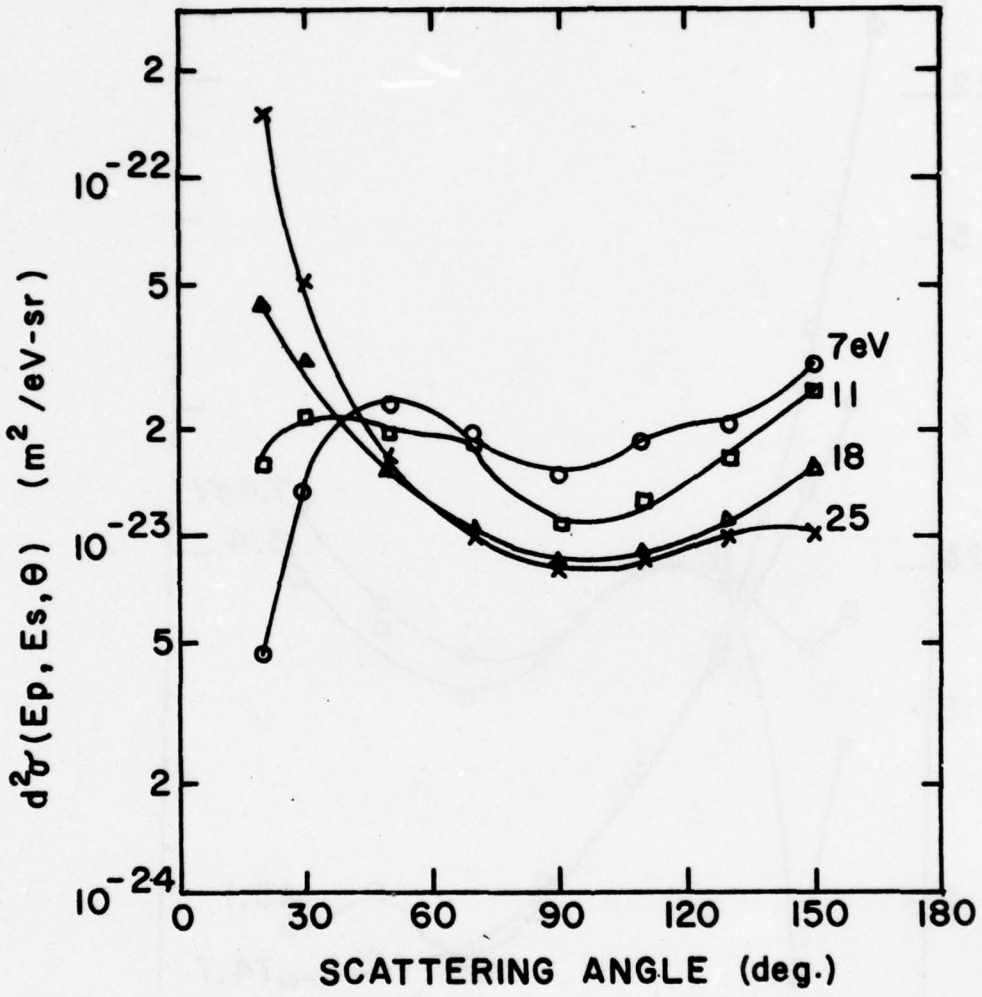

Figure 4. 50 eV e^- on Helium, Ejected and Inelastically Scattered Electrons.

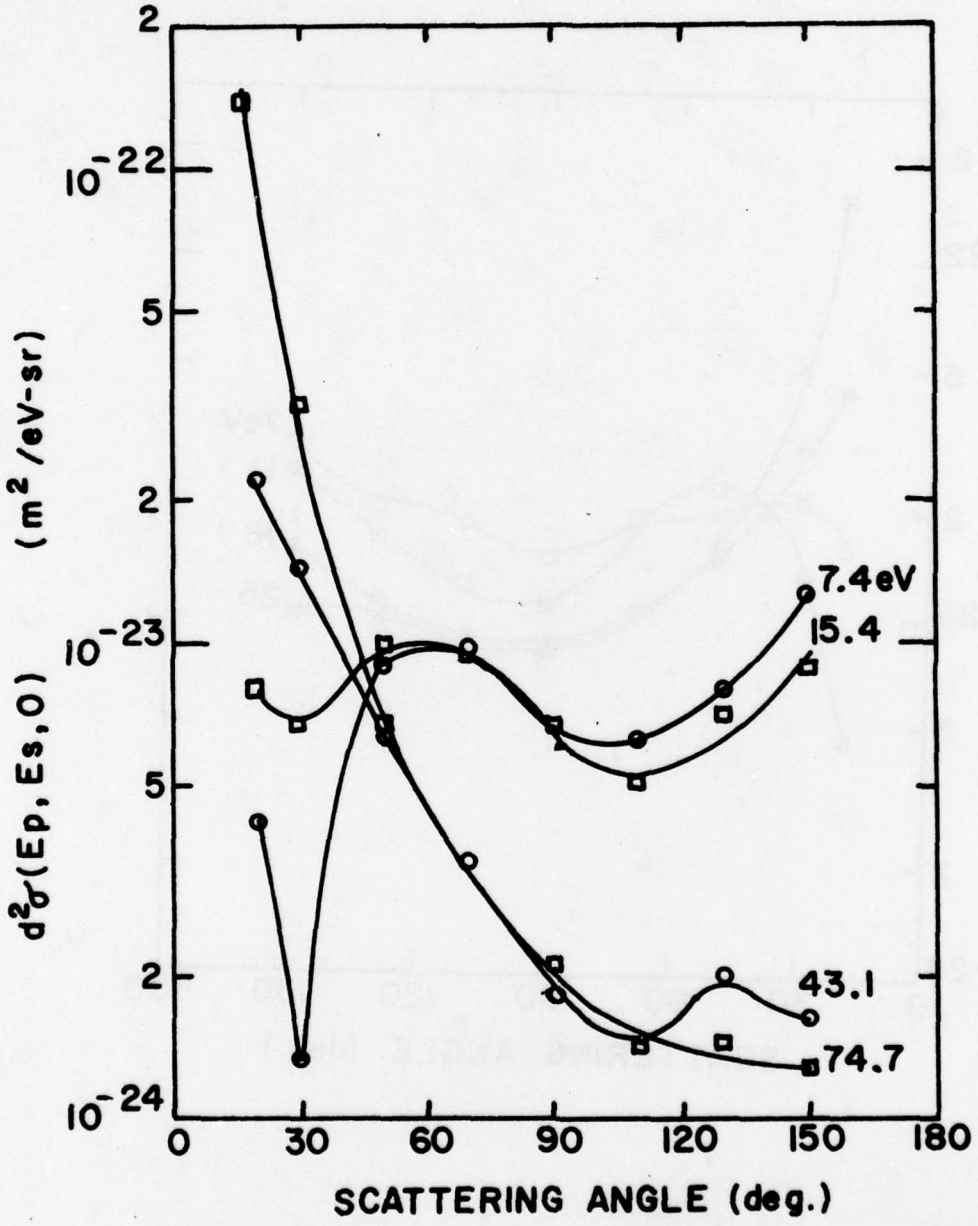

Figure 5. Angular Dependence of Ejected and Inelastically Scattered Electrons for 100 eV e^- on Helium.

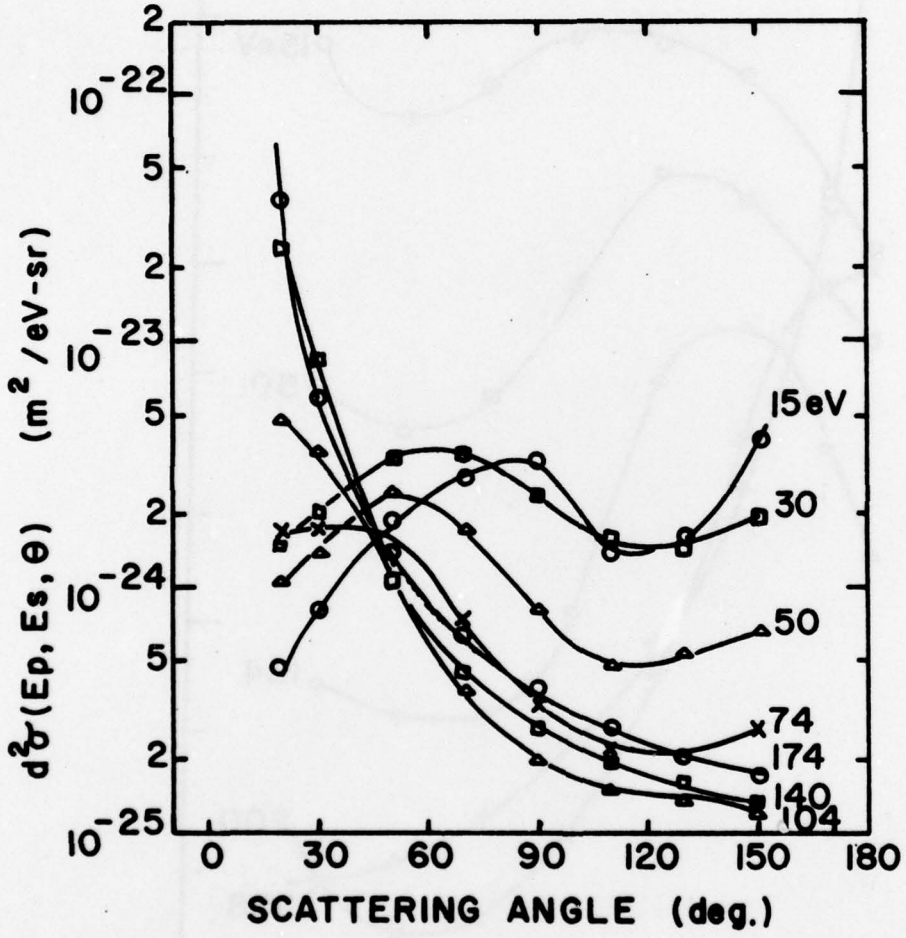

Figure 6. 200 eV e^- on Helium, Ejected and Inelastically Scattered Electrons.

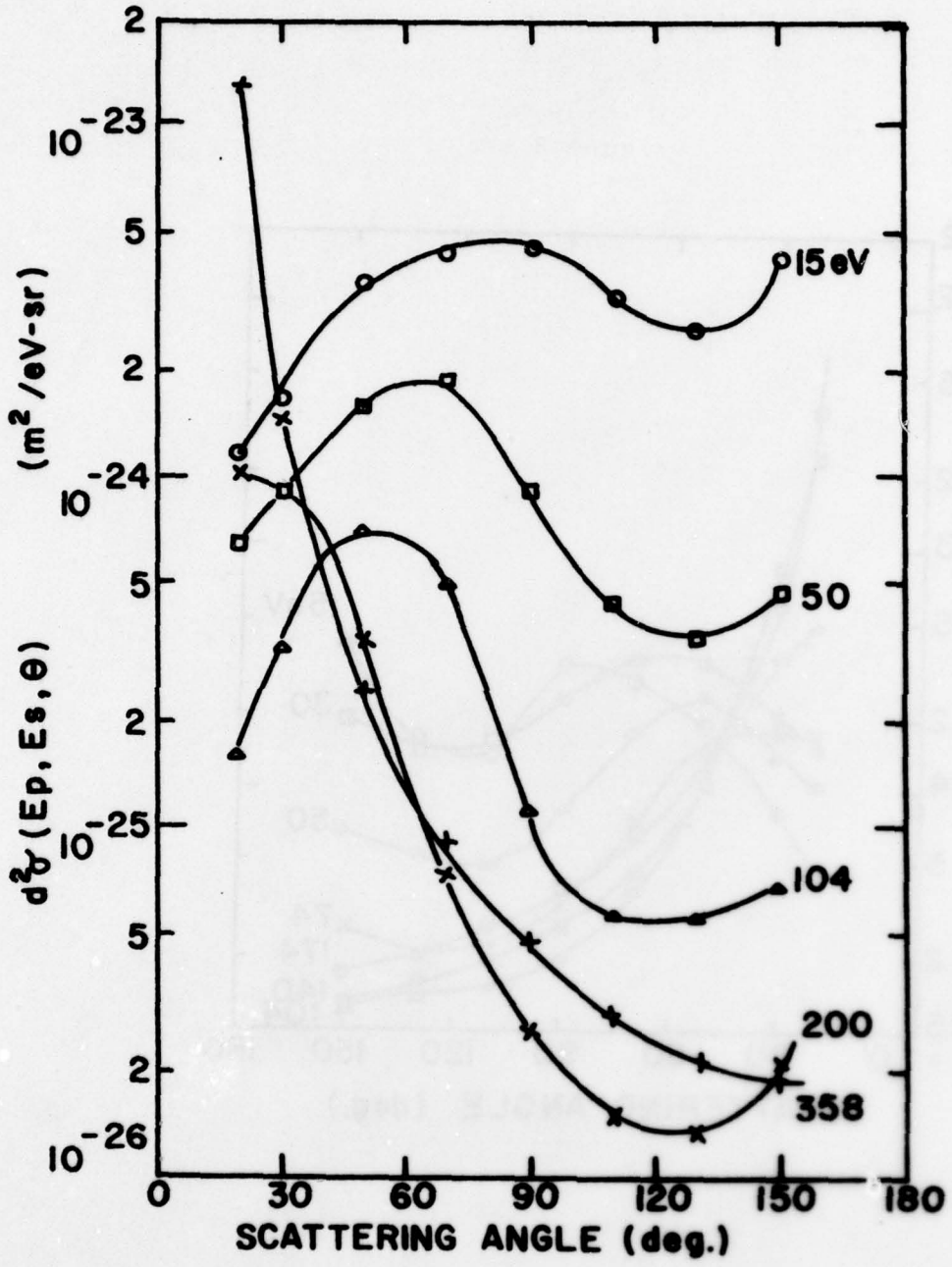

Figure 7. 400 eV e^- on Helium, Ejected and Inelastically Scattered Electrons.

citation collision, Figure 2 shows the differential cross-sections for 50 eV electrons producing 2^1S, 2^3S, 2^1P and 2^3P states of the helium atom. The important fact to note is that, indeed, the cross-sections are forward peaked ($\theta \simeq 0°$), but assume a lower value in the lateral direction than the backscatter direction. Figure 3 shows the similar tendency for 100 eV electrons. Figures 4 to 6 illustrate the nature of the angular dependence of doubly differential cross-section for an ionizing collision. For the same species (He), we present the angular differential cross-sections as obtained experimentally by Peterson et al (1971, 1972). These are shown in Figures 8 and 9. There exists a considerable amount of experimental data (c.f. Lassettre et al, 1964a, b, 1968) which can be used for constructing a realistic angular model of scattering for the purpose of calculating the photoelectron fluxes in the upper atmosphere.

The assumption that the photoelectrons below about 10 eV are isotropically scattered by neutrals is fairly accurate. However, this assumption is not valid for the Coulomb interaction. When the energy of an electron has degraded below about 15 eV, the Coulomb interactions with ambient thermal plasma begin to play an important role. For higher energy electrons (about about 15 eV), Spitzer's (1956) model of small angle scattering (by plasma) may be deemed satisfactory. Along the same line, further developments by Butler and Buckingham (1962) and the empirical model by Swartz et al (1971) for the rate of energy loss (see Figure 10) are indispensable for modelling. However, below 10 eV at closer examination of the pitch angle scattering by the thermal plasma is essential. In view of the fact that the maximum heating rate of the ambient plasma by hyperthermal electrons occurs in the neighborhood of 2 to 3 eV (except for ^1O_D (6300Å), ^1O_S (5577Å) and vibrational states of N_2) the escape rate of soft electrons, for instance, to the dark side of the magnetically

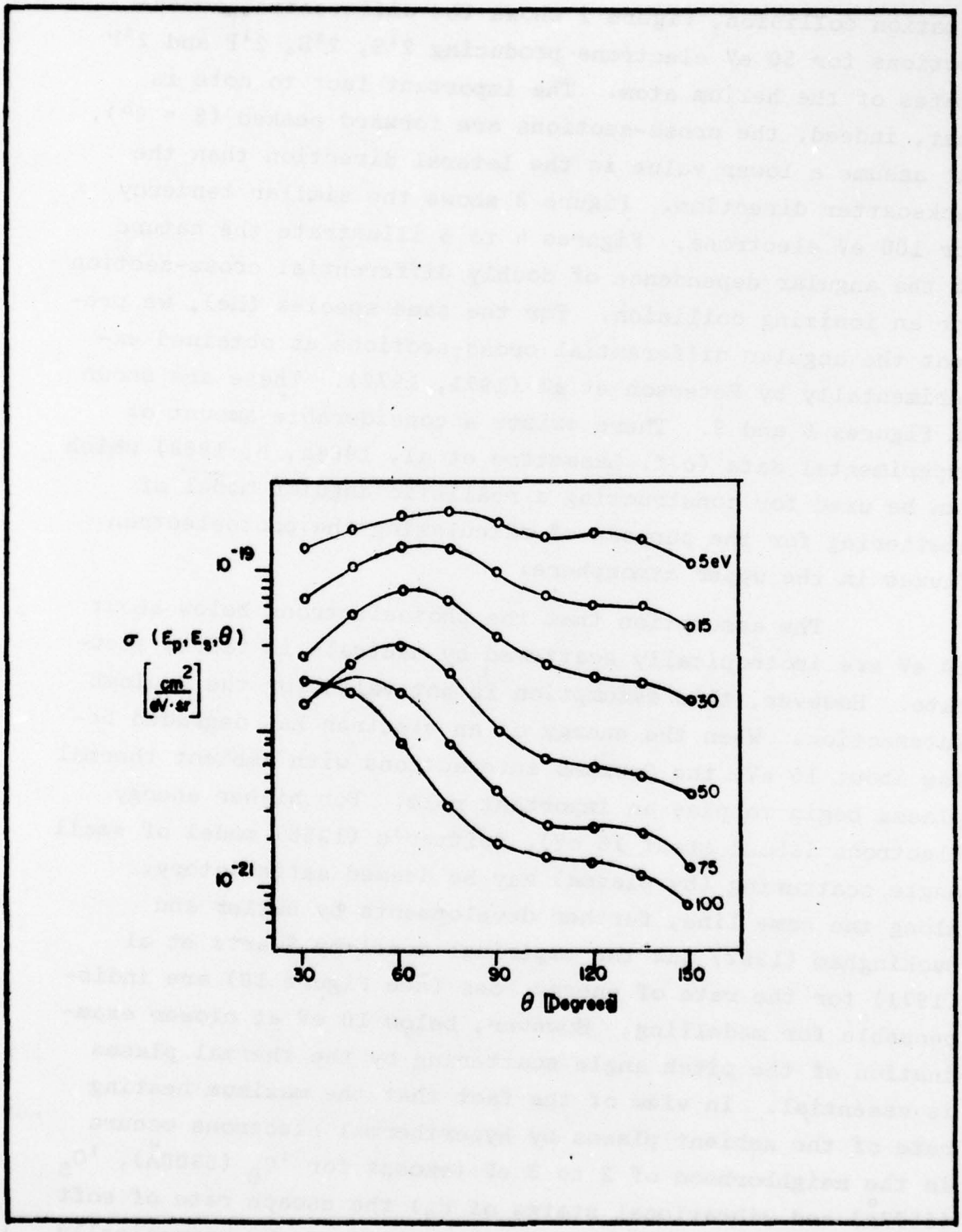

Figure 8. Double Differential Cross-Section, σ(Ep, Es, θ) for Ep = 200 eV and Selected Values of Secondary Energy.

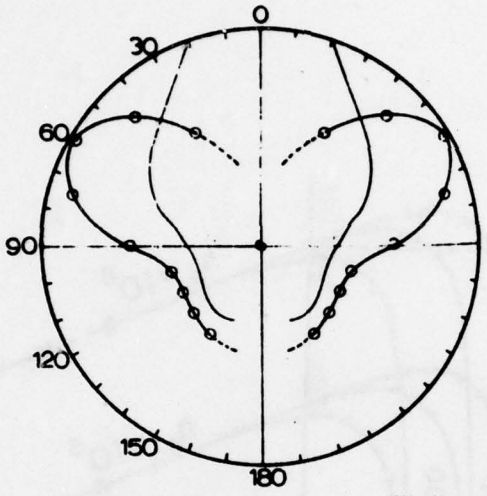

Figure 9. Angular Distribution of 23 eV Electrons Ejected From Helium by 100 eV Electrons.

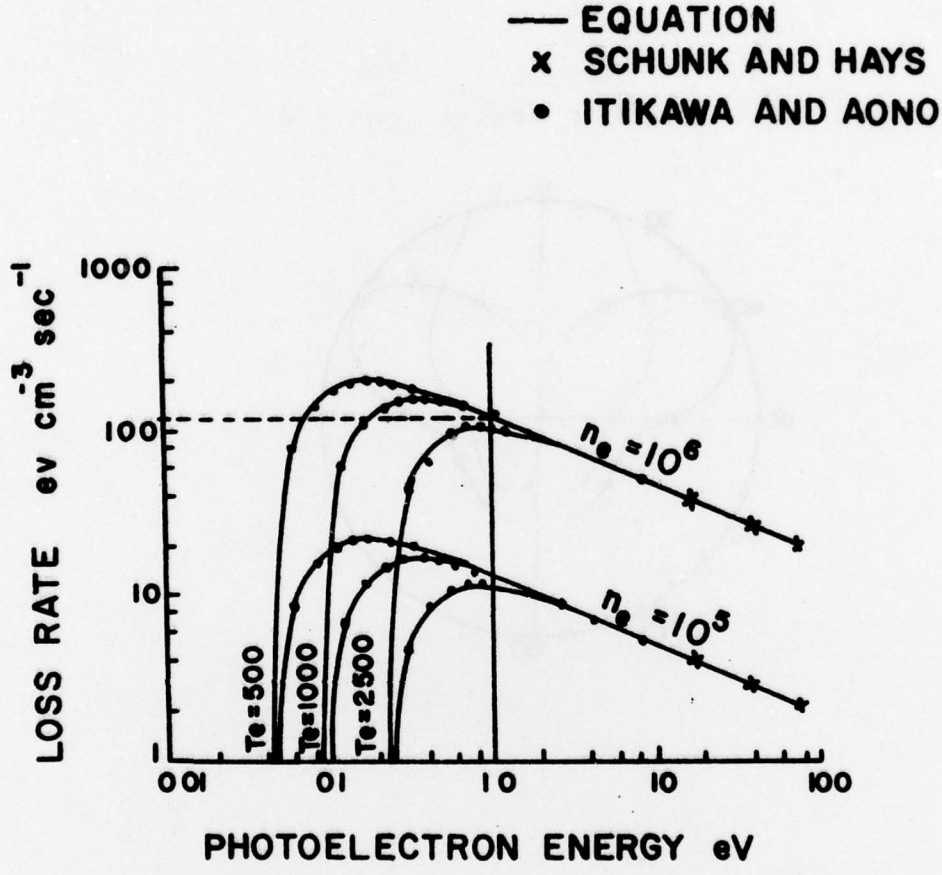

Figure 10. Comparison of Energy-Transfer Rates for Photoelectrons Interacting with Thermal Electrons.

conjugate ionosphere is determined by the ambient plasma. In fact, for high invariant latitudes, the escaping electrons from the lower ionosphere (~250 km) travel through either the trough or the plasmasphere, where the main interaction is electron-plasma, before reaching the conjugate dark side. The part of the study here was to develop a realistic model of such an interaction and incorporate that in the transport calculations. To this end, it was discovered by this author that the electron transport equation (see Eq. (17)) could be solved (and was solved) by a variational principle combined with the Green's function approach. The angular differential cross-sections could then be incorporated as an empirical fit to the data points. The use of the Green's function was made to set up the boundary-value problems for the three regions of the upper atmosphere. Another point of importance which was deemed absolutely necessary, was, to account for the transport of electrons in the regions of large magnetic dip angles (for instance the auroral oval and the polar region). This was due to the fact that the atmospheric density profile changed as a function of altitude and thus presented an inhomogeneous interacting medium. Thus far, we have been able to account for the inhomogeneity only under the approximation that within about two mean free paths of electrons the fractional abundance of various species can be approximated by a local mean value. For altitudes above the perigee of INJUN5 satellite (~660 km) this approximation is good. Between 250-600 km is the transition region where a great deal of care is required to accurately calculate the collision rates of hyperthermal electrons as a function of their relaxation lengths. Below 250 km, the so called "local hypothesis" is fairly valid, i.e. the hyperthermal electrons are essentially thermalized in the localized region so that the transport effects can be neglected. As a final point regarding our task, electric and magnetic fields were incorporated in the calculations (see Eq. (19)). By the very nature of the Lorentz force term, the

resulting $\underset{\sim}{E} \times \underset{\sim}{B}$ drifts and the loss of the azimuthal symmetry of the spiralling motion of electrons makes the problem of multi-dimensions both in the spatial and the momentum coordinates. We have succeeded to some extent in simplifying the transport equation by various transformations. However, a complete theory is not available yet.

To summarize our contributions to the AFGL project on the morphology of the electron transport, our performance for the net period of four months is as follows:

1) For a linearly anisotropic pitch angle scattering we have a complete set of transport models for the temperate, the precipitation and the polar region. Of these the computer program for the temperate zone has been given to the Electrical Processes Branch (R. C. Sagalyn) of AFGL. The program needs to be debugged. However, two subroutines in that program, which calculate the electron impact secondary ionization and the continuous rate of energy loss of hyperthermal electrons to the cool ambient plasma, are debugged and working.

2) A discovery was made that a variational principle can be used (and was used) to treat the realistic form of the pitch angle scattering in the transport calculations. A paper is being written on that application and will be submitted to a suitable journal.

3) Study has been initiated to incorporate electric and magnetic fields in the transport phenomenon.

4) In cooperation with R. C. Sagalyn of AFGL, Drs. William Burke and Lalita Rao (of Regis College), INJUN5 data was analyzed for the study of SAR arcs and the electron heating in the conjugate dark side

of the ionosphere by the photoelectrons transported from the sunlit side. Abstracts of two papers submitted to the J. Geophys. Res. (1977) are given below.

4.0 ABSTRACTS OF PAPERS SUBMITTED

INJUN 5 LOW-ENERGY PLASMA OBSERVATIONS DURING A MAJOR MAGNETIC STORM

Electron densities and temperatures as well as the omnidirectional flux of positive ions with E > 28 eV were measured by the spherical Langmuir probes aboard Injun 5 at altitudes greater than 2000 km during the October-November 1968 geomagnetic storm period. During the early phases of the storm, the electron density in the trough decreased and the temperature increased. As the storm progressed, the position of the trough moved equatorward. Plasma erosion was observed to the invariant latitude of 40° during the early recovery phase. The latitude of the transition between light and heavy ion dominance also moved equatorward, but recovered at a slower rate than the position of the electron trough. Most of the hyperthermal ions measured near the trough were due to ring-current particles reaching to the satellite's altitude. The minimum electron densities in the trough were measured to be within 1° of latitude of the maximum ion flux. The maximum electron temperatures were observed several degrees equatorward of the maximum ion flux. At the reported time and latitude of an SAR arc, an electron temperature of about 4700°K was observed, whereas in the absence of the ring-current, a temperature of about 2000°K would be expected. The observations are also used to evaluate a method for calculating the position of ring current using magnetic fluctuations observed at ground level.

THERMAL AND HYPERTHERMAL ELECTRON DISTRIBUTIONS IN THE MIDNIGHT SECTOR OF THE WINTER TOPSIDE IONOSPHERE

A gridded spherical electrostatic analyzer aboard Injun 5 has been used to measure fluxes of thermal and hyperthermal electrons at sub-auroral altitudes in the midnight sector of the northern ionosphere between altitudes of 2500 and 850 km. Hyperthermal fluxes, consisting of energetic photoelectrons that have escaped from the sunlit southern hemisphere are observed along orbits over the Atlantic Ocean and North America but not over Asia. The electron temperatures near 2500 km have their highest values at trough for all longitudes. In the longitude sector to which conjugate photoelectrons have access, $T_e \sim 4000°K$ at 2500 km and $\sim 3000°K$ at 1000 km. For regions with the conjugate point in darkness $T_e \simeq 2300°K$ over the 1000-2500 km altitude range. Effective spectral characteristics of the photoelectrons are studied as functions of latitude and altitude. Based on these observations, it is concluded that: (1) Conjugate photoelectrons are not the major contributors to trough heating; (2) Heat conduction rather than local heating by conjugate photoelectrons is responsible for electron temperature distributions observed in regions with sunlit conjugate points.

5.0 REFERENCES

Burke, W. J., R. C. Sagalyn and M. Kanal (1977): Thermal and hyperthermal electron distributions in the midnight sector of the winter topside ionosphere (submitted to J. Geophys. Res. 1977).

Rao, L. D. V., W. J. Burke, M. Kanal and R. C. Sagalyn (1977): Injun 5 low-energy plasma observations during a major magnetic storm (submitted to J. Geophys. Res. 1977).

Opal, C. B., W. K. Peterson and E. C. Beaty (1971), J. Chem. Phys., 55, 4100.

McCormick, N. J. and I. Kuscer (1965), J. Math. Phys., 6, 1939.

Case, K. M. and P. F. Zweifel (1967): Linear transport theory, Addison-Wesley, Reading, Massachusetts.

Mika, J. R. (1961), Nucl. Sci. Eng., 11, 415.

Zelazny, R., A. Kuskell and J. Mika (1961), Ann. Phys., 16, 69.

Kanal, M. (1970), J. Math. Phys., 11, 3042.

Crooks, G. B. and M. E. Rudd (1972): Energy and angular distributions of scattered and ejected electrons produced by 500-800 eV electrons in helium, Ph.D. Thesis, University of Nebraska, Lincoln, Nebraska.

Peterson, W. K., C. B. Opal and E. C. Beaty (1971), J. Phys. B, Atom. Molec. Phys., 4, 1020.

Peterson, W. K., E. C. Beaty and C. B. Opal (1972), Phys. Rev., A5, 713.

Lassettre, E. N., A. S. Berman, S. M. Silverman and M. E. Krasnow (1964a), J. Chem. Phys., 40, 1232.

Lassettre, E. N. and M. E. Krasnow (1964b), J. Chem. Phys., 40, 1248.

Lassettre, E. N., A. Skerbele, M. A. Dillon and K. J. Ross (1968), J. Chem. Phys., 48, 5066.

Spitzer, L., Jr. (1956): Physics of fully ionized gases, Interscience Publishers, Inc., New York.

Butler, S. T. and M. J. Buckingham (1962), Phys. Rev. Second Series, 126, No. 1, 1.

Swartz, W. E., J. S. Nisbet and A. E. S. Green (1971), J. Geophys. Res., 76, 8425.